256-QAM Modem Performance in Distorted Channels

KUANG-TSAN WU AND KAMILO FEHER

Abstract—**Performance degradations of 256-QAM modems in distorted channels are studied in this correspondence. Illustrative linear, parabolic, and sinusoidal amplitude and group delay channel distortions, caused by filter imperfections and/or by selective radio fades, are investigated. To enable an easy comparison with 64-QAM systems, we present the degradations of these systems in the same figures as those of 256-QAM modems. It is shown that linear (slope) group delay and sinusoidal (ripple) amplitude distortions cause the most significant performance degradations.**

I. Introduction

Digitial 64-QAM radio systems are described in many references, including [1]-[4], [7]-[10]. The theoretical RF spectral efficiency of 64-QAM systems is 6 bits/s/Hz. With $\alpha = 0.3$–0.5 rolloff raised-cosine Nyquist channel filters [7], [10] a practical spectral efficiency of 6 bits/s/Hz $\div (1 + \alpha) = 4.5$ bits/s/Hz has been achieved. Due to the increasing need for even higher bandwidth efficiency digital radio and hybrid data-under-voice (DUV), data-in-voice (DIV), and data-above-voice/video (DAV) systems [7], we consider 256-QAM as a next logical step. An $\alpha = 0.2$ raised-cosine filtered 256-QAM modem could achieve a practical efficiency of 8 bits/s/Hz $\div$ 1.2 = 6.66 bits/s/Hz. For example, such a high spectral efficiency is required for the DIV transmission of a 1.544 Mbit/s rate signal in the standard analog supergroup band of 240 kHz.

Although it is known that the sensitivity of higher order modulation techniques to different impairments may increase significantly with the number of states, the performance of 256-QAM under various effects such as channel distortions is not yet available in the literature. The objective of this paper is to investigate the effect of channel fading and/or hardware imperfections on 256-QAM. The structure of 256-QAM and the computer simulation model are briefly described. The effects of group delay and amplitude distortions with linear, parabolic, or sinusoidal characteristics on 256-QAM are evaluated. Measured 256-QAM eye diagrams which confirm our computer simulation results are also included.

II. Analysis and Description of Computer Simulations

Fig. 1 shows a block diagram of a 256-QAM system. The modulated 256-QAM signal can be represented by (1)

$$s(t) = \mathrm{Re}\left[\sum_{n=0}^{\infty} (I_n + jQ_n) g(t - nT_s) e^{j2\pi f_0 t}\right] \tag{1}$$

where

Re [ ] denotes real part of

f_0 is the carrier frequency
$1/T_s$ is the symbol rate; for 256-QAM, $T_s = 8T_b$
$1/T_b$ is the bit rate
$g(t)$ is a pulse defined by

$$g(t) = \begin{cases} 1 & \text{if } 0 \leqslant t \leqslant T_s \\ 0 & \text{elsewhere} \end{cases}$$

I_n and $Q_n = \pm 1, \pm 3, \cdots, \pm 15$ are the sampled values of the in-phase and quadrature symbols.

The simulation is performed entirely in the complex baseband form as shown in Fig. 2. We report simulation results for systems having a symbol rate of 15 Mbaud (120 Mbits/s). The choice of this baud rate is for an easy comparison with the performance 90 Mbit/s rate 64-QAM systems. The results can be applied to another bit rate by appropriate scaling. In the simulation a perfect carrier and symbol timing is assumed. For filtering we use FFT techniques to alternate between the frequency and time domains. The assumed PRBS sequence length is 16 384 bits. The number of samples per symbol is 32.

The transmit and receive filters are assumed as the ideal square root of raised-cosine filters with $x/\sin(x)$ equalization in the transmitter, so that the whole system satisfies the Nyquist first criterion [7], [10]. The resulting eye diagrams for $\alpha = 0.1$ and 0.4 are shown in Fig. 3(a) and (b) where α denotes the rolloff factor, that is, the ratio of the excess bandwidth to the Nyquist band. The eye diagram of an $\alpha = 0.2$ unequalized channel, having a sinusoidal group delay distortion, is illustrated in Fig. 3(c). Illustrative measurement results are shown in Fig. 4.

Note that for the ideal filter there is no ISI at the optimum sampling instant. However, data transition jitter is very significant, particularly in the $\alpha = 0.1$ filtered case. This indicates that a high-precision sampling clock is required.

For specified power of white Gaussian noise at the threshold detector input, the error probability of the ith symbol with respect to the in-phase channel is calculated as follows:

$$P_{S_i}{}^I = \begin{cases} \dfrac{1}{2}\,\mathrm{erfc}\left(\dfrac{|\bar{S}_i - \mathrm{THR1}_i|}{\sqrt{2}\sigma}\right), & \text{for } I_i = \pm 15 \\ \dfrac{1}{2}\,\mathrm{erfc}\left(\dfrac{|\bar{S}_i - \mathrm{THR1}_i|}{\sqrt{2}\sigma}\right) + \dfrac{1}{2}\,\mathrm{erfc}\left(\dfrac{|\mathrm{THR2}_i - \bar{S}_i|}{\sqrt{2}\sigma}\right), & \text{for } I_i = \pm 1, \pm 3, \cdots, \pm 13 \end{cases} \tag{2}$$

where I_i is the ith transmitted symbol of the in-phase channel, $\bar{S}_i$ is the magnitude of the ith received sample of the in-phase channel,

$$\mathrm{THR1}_i = |I_i| - 1; \quad \mathrm{THR2}_i = |I_i| + 1;$$

$$\mathrm{erfc}\,(x) \triangleq \frac{2}{\sqrt{\pi}} \int_x^{\infty} e^{-t^2}\, dt$$

and σ^2 is the received noise power at the threshold detector input. The error probability $P_{s_i}{}^Q$ with respect to the quadrature channel is obtained similarly from (2), and for a sequence of N symbols in each channel, the average symbol error rate P_s is calculated as follows:

$$P_s = 1/N \sum_{i=1}^{N} \cdot \frac{1}{2} (P_{s_i}{}^I + P_{s_i}{}^Q). \tag{3}$$

Paper approved by the Editor for Radio Communication of the IEEE Communications Society for publication without oral presentation. Manuscript received May 11, 1984; revised October 18, 1984. This work was supported by the Natural Sciences and Engineering Research Council (NSERC) of Canada and by Karkar Electronics, Inc., San Francisco, CA.

K. -T. Wu is with the Department of Electrical Engineering, University of Ottawa, Ottawa, Ont., Canada K1N 6N5, on leave from The National Taiwan University, Taipei, Taiwan, Republic of China.

K. Feher is with the Department of Electrical Engineering, University of Ottawa, Ottawa, Ont., Canada K1N 6N5, and with Stanford University, Stanford, CA 94305.

DOCKET ALARM Find authenticated court documents without watermarks at docketalarm.com.

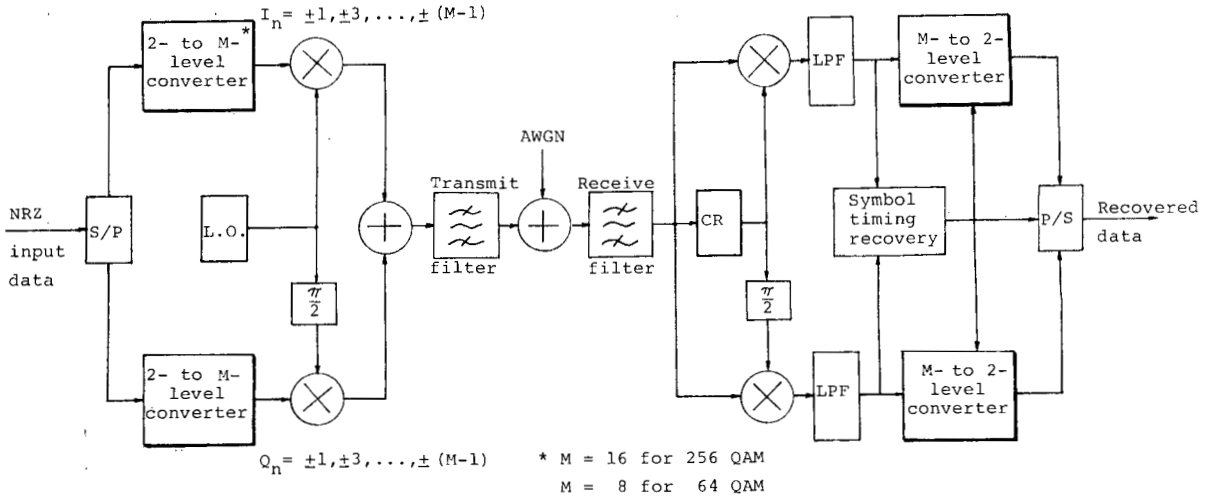

Fig. 1. 256 and/or 64 QAM system block diagram.

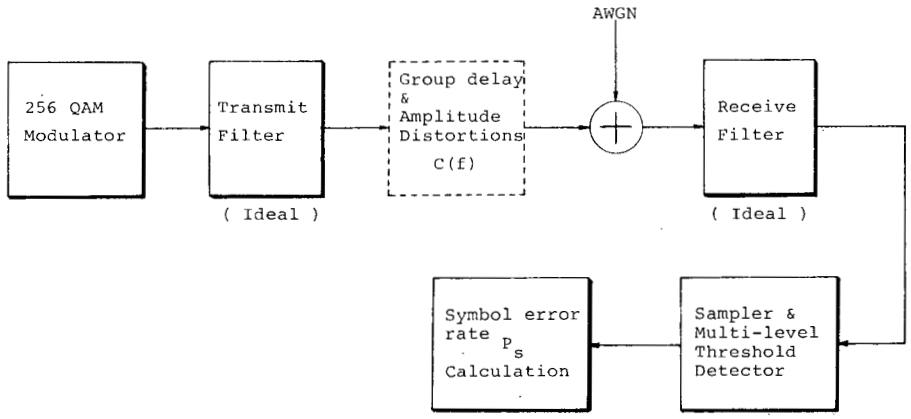

Fig. 2. Computer simulation model of 256-QAM and 64-QAM systems.

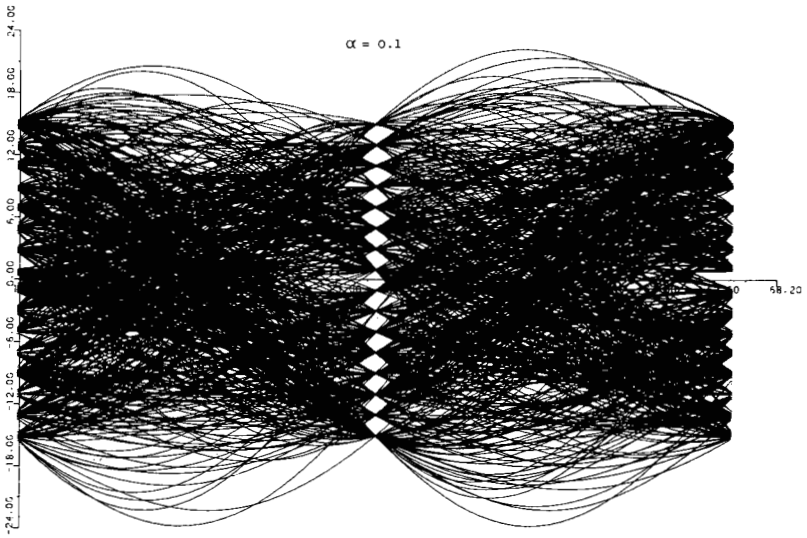

(a)

Fig. 3. Eye diagrams of 256-QAM. (a) $\alpha = 0.1$, (b) $\alpha = 0.4$, (c) $\alpha = 0.2$ with sinusoidal group delay distortion, $D(f) = S_0 \sin(2\pi Kf/2f_{BW})$, $S_0 =$

DOCKET ALARM Find authenticated court documents without watermarks at docketalarm.com.

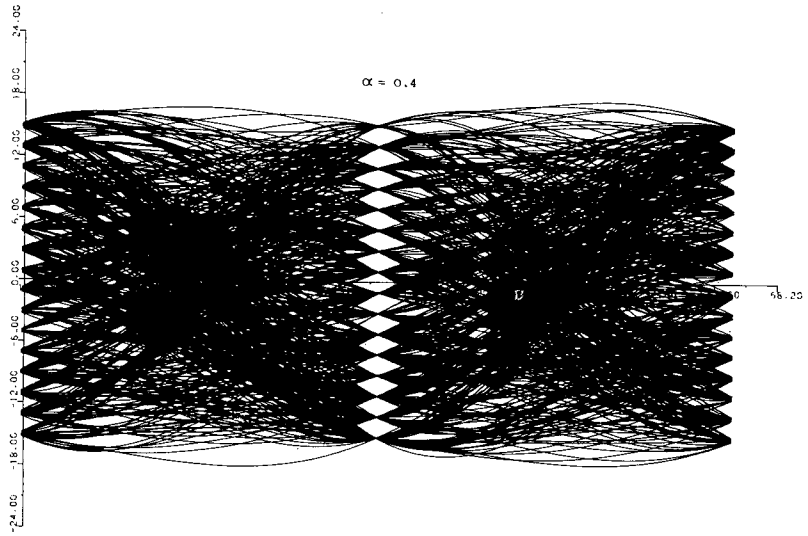

(b)

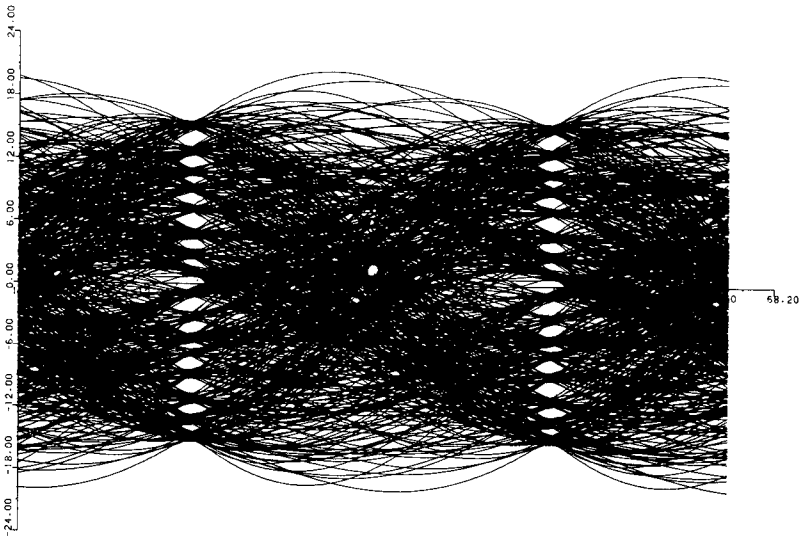

(c)

Fig. 3. (*Continued*).

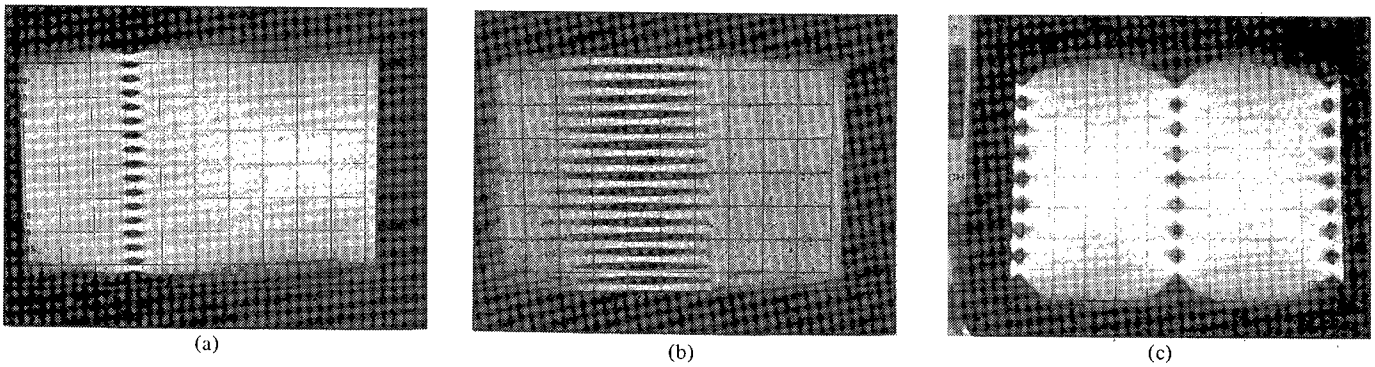

(a) (b) (c)

Fig. 4. Measured 256-QAM and 64-QAM demodulated *I*-channel eye diagrams. *I*-channel symbol rate f_s = 200 kbaud corresponds to modem bit rate of 1.6 Mbits/s (256-QAM) and 1.2 Mbits/s (64-QAM). Raised cosine channel Nyquist filters (f_N = 100 kHz) having a rolloff parameter α = 0.2 and a 55 dB attenuation beyond 120 kHz, designed by Karkar Electronics, Inc., are used in this experiment. Unequalized filters have a

DOCKET ALARM Find authenticated court documents without watermarks at docketalarm.com.

III. Group Delay Distortions

To investigate the effects of selective fading and/or radio system hardware imperfections, we insert between the transmit and the receive filters a linear filter with the equivalent baseband transfer function $C(f)$, as shown in Fig. 2. We may express the frequency response $C(f)$ as

$$C(f) = |C(f)|e^{j\theta(f)} \tag{4}$$

and

$$A(f) = C(f) \tag{5}$$

$$D(f) = \frac{-1}{2\pi}\frac{d\theta(f)}{df}. \tag{6}$$

To simulate the group delay distortion we assume there is no amplitude distortion, i.e., $A(f) = 1$. The group delay distortions are defined as follows:

$$D(f) = \begin{cases} L_D \cdot f & \text{for linear group delay} \\ P_D \cdot f^2 & \text{for parabolic group delay} \\ S_D \cdot \sin(2\pi Kf/2f_{BW}) & \text{for sinusoidal group delay} \end{cases} \tag{7}$$

where

$$f_{BW} \triangleq (1+\alpha)f_N$$

and f_N is the Nyquist bandwidth in baseband. This $(1+\alpha)f_N$ bandwidth definition (for group delay distortion) is more appropriate than f_N, as it includes the critical effect of the group delay at the edge of the filter attenuation band. In the case of sinusoidal group delay, we present only results for $K = 4$. The symbol error rate P_s versus average C/N is computed. Typical results are shown in Fig. 5. We define a maximum group delay τ_m in the filter bandwidth $(2f_{BW})$ as follows:

$$\tau_m \triangleq \begin{cases} L_D(2f_{BW}) \text{ ns} & \text{for linear group delay} \\ P_D(f_{BW})^2 \text{ ns} & \text{for parabolic group delay} \\ S_D \text{ ns} & \text{for sinusoidal group delay.} \end{cases} \tag{8}$$

The degradation of C/N as a function of τ_m relative to the case with no distortion, for P_s of 10^{-4}, is shown in Fig. 6. Note that here we simulate a 120 Mbit/s system with $\alpha = 0.4$. We also include the performance of a 90 Mbit/s 64-QAM system with $\alpha = 0.4$ in Fig. 6, which is confirmed to be the same as in [1]. Again we notice that for a given value of maximum group delay τ_m in the filter bandwidth, linear group delay causes the most severe degradation to the system's performance as compared to parabolic or sinusoidal group delay distortions [1].

IV. Amplitude Distortions

For the simulation of the amplitude distortion, we assume the group delay distortion is equalized, i.e., $D(f)$ is equal to a constant. Three different characteristics for the amplitude distortion are defined as follows:

$$A(f) = \begin{cases} L_A \cdot f & \text{for linear amplitude distortion} \\ P_A \cdot f^2 & \text{for parabolic amplitude distortion} \\ S_A \cdot \sin(2\pi Kf/2f_{BW}) & \text{for sinusoidal amplitude} \end{cases}$$

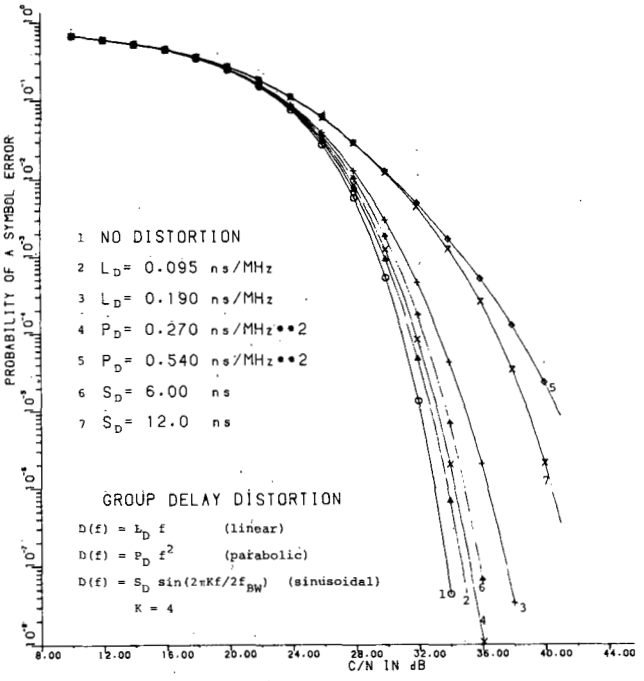

Fig. 5. P_s versus C/N for linear, parabolic, and sinusoidal group delay distortions for 256-QAM with a bit rate of 120 Mbits/s, i.e., 15 Mbaud and $\alpha = 0.4$. Noise is defined in the double-sided Nyquist bandwidth, i.e., the equivalent noise bandwidth is 15 MHz.

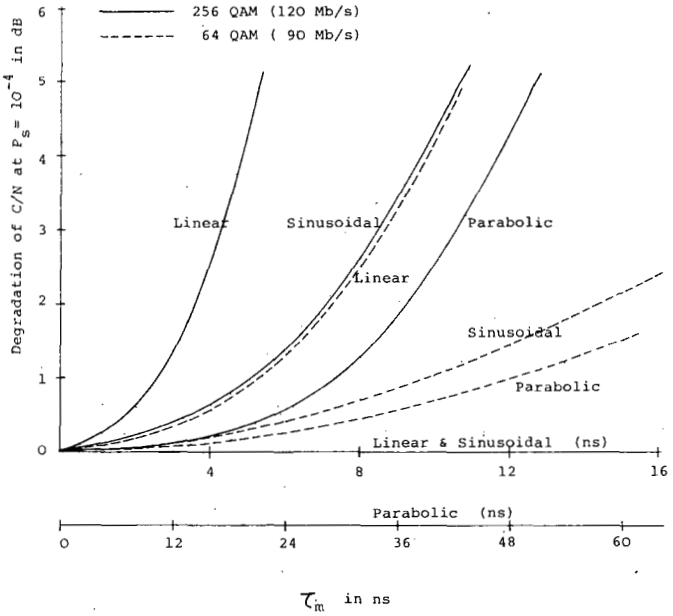

Fig. 6. Degradation of C/N versus τ_m for linear, parabolic, and sinusoidal group delay distortions for 256-QAM and 64-QAM with symbol rate of 15 Mbaud and $\alpha = 0.4$ raised-cosine filters, where

$\tau_m = L_D(2f_{BW})$ ns (linear)
$= P_D(f_{BW})^2$ ns (parabolic)
$= S_D$ ns (sinusoidal)
$f_{BW} = (1+\alpha) = 1.4f_N = 10.5$ MHz.

DOCKET ALARM Find authenticated court documents without watermarks at docketalarm.com.

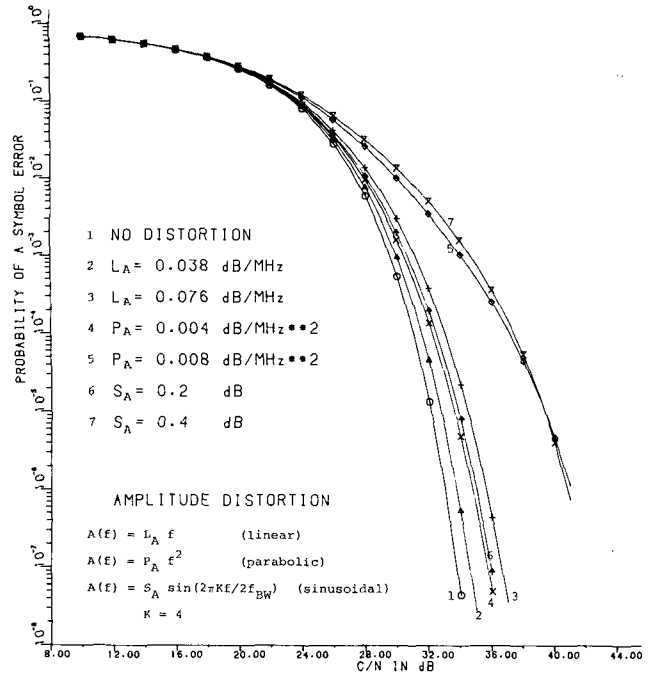

Fig. 7. P_s versus C/N for linear, parabolic, and sinusoidal amplitude distortions for 256-QAM with a bit rate of 120 Mbits/s, i.e., 15 Mbaud and $\alpha = 0.4$. Noise is defined in the double-sided Nyquist bandwidth, i.e., the equivalent noise bandwidth is 15 MHz.

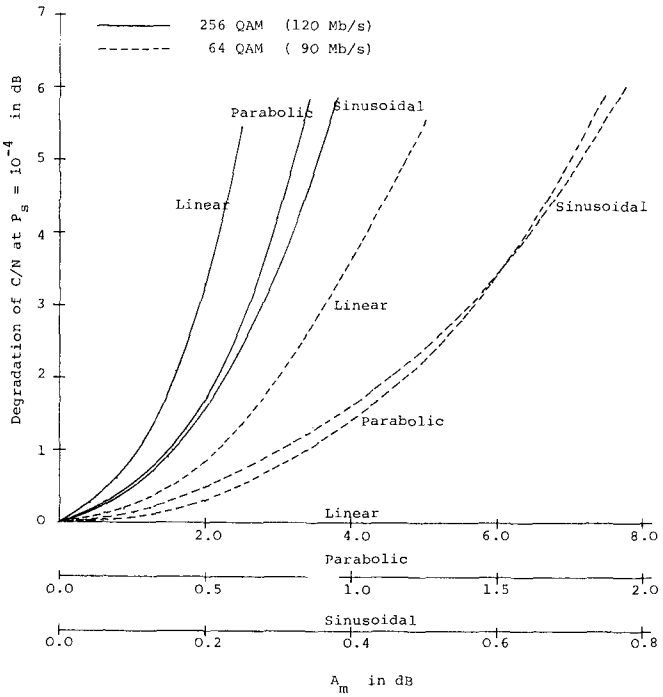

Fig. 8. Degradation of C/N versus A_m for linear, parabolic, and sinusoidal amplitude distortions for 256-QAM and 64-QAM with symbol rate of 15 Mbaud and $\alpha = 0.4$ raised-cosine filters, where

$$\begin{aligned} A_m &= L_A(2f_{BW}) && \text{(linear)} \\ &= P_A(f_{BW})^2 && \text{(parabolic)} \\ &= S_A && \text{(sinusoidal)} \end{aligned}$$

$f_{BW} = (1 + \alpha)f_N = 1.4f_N = 10.5$ MHz.

The symbol error rate P_s versus C/N is computed. A typical result is shown in Fig. 7. Degradations of C/N for 256-QAM and 64-QAM with 15 Mbaud and $\alpha = 0.4$, versus maximum amplitude distortion A_m in the filter bandwidth, are plotted in Fig. 8, where

$$A_m \triangleq \begin{cases} L_A(2f_{BW}) & \text{for linear amplitude distortion} \\ P_A(f_{BW})^2 & \text{for parabolic distortion} \\ S_A & \text{for sinusoidal distortion.} \end{cases} \quad (10)$$

We note that for a given value of maximum amplitude distortion (A_m), linear amplitude distortion causes the least degradation, followed in order of increasing degradation by parabolic and sinusoidal amplitude distortions.

V. Conclusion

The effects of amplitude and group delay distortions on the error performance on 256-QAM have been studied. Computer simulation and measurement results indicate that linear group delay distortion is the most critical group delay parameter.

References

[1] T. Hill and K. Feher, "A performance study of NLA 64-state QAM," *IEEE Trans. Commun.*, vol. COM-31, pp. 821–826, June 1983.
[2] M. Borgne, "Comparison of 16, 32, 64 and 128 QAM modulation schemes for digital radio systems," presented at IEEE GLOBECOM, San Diego, CA, 1983.
[3] B. T. Bynum and E. W. Allen, "135 Mb/s—6 GHz transmission system design considerations," presented at IEEE Int. Conf. Commun., Boston, MA, 1983.
[4] T. Noguchi, T. Ryu, and Y. Koizumi, "6 GHz 135 MBPS digital radio system with 64 QAM modulation," presented at IEEE Int. Conf. Commun., Boston, MA, 1983.
[5] M. Subramanian, K. C. O'Brien, and P. J. Puglis, "Phase dispersion characteristics during fade in a microwave line-of-sight radio channel," *Bell Syst. Tech. J.*, vol. 52, Dec. 1973.
[6] G. M. Babler, "Selectively faded nondiversity and space diversity narrowband microwave radio channels," *Bell Syst. Tech. J.*, vol. 52, Feb. 1973.
[7] K. Feher, *Digital Communications: Microwave Applications*. Englewood Cliffs, NJ: Prentice-Hall, 1981.
[8] Y. Saito, S. Komaki, and M. Murotani, "Feasibility considerations of high level QAM multi-carrier system," presented at IEEE Int. Conf. Commun., Amsterdam, The Netherlands, 1984.
[9] J. D. McNicol, S. G. Barber, and F. Rivest, "Design and application of the RD-4A and RD-6A 64-QAM digital radio systems," presented at IEEE Int. Conf. Commun., Amsterdam, The Netherlands, 1984.
[10] K. Feher, *Digital Communications: Satellite/Earth Station Engineering*. Englewood Cliffs, NJ: Prentice-Hall, 1983.

On Variable Length Codes Under Hardware Constraints

HAIM GARTEN

***Abstract*—A method for finding a variable length code set under the constraint of maximal clock rate is presented. Given a probability vector and requiring that the length of codewords would be an integer multiple of some K ($K>2$) reduces the maximal clock rate needed in implementing the compression system. On the other hand, given a maximal clock rate, the method enables us to use a quantizer with more levels than the usual**

Paper approved by the Editor for Signal Processing and Communication Electronics of the IEEE Communications Society for publication without oral presentation. Manuscript received February 17, 1984; revised August 15, 1984.

The author is with Rafael, State of Israel, Haifa, Israel.

0090-6778/85/0500-0491$01.00 © 1985 IEEE

DOCKET ALARM Find authenticated court documents without watermarks at docketalarm.com.